11-2020

Ion Pairing versus Solvation of Dinitrobenzene Anions in Room-Temperature Ionic Liquids (RTILs): Vibrational Signatures of RTIL–Substrate Interactions

Abderrahman Atifi
Marquette University

Piotr J. Mak
Marquette University, piotr.mak@marquette.edu

Michael D. Ryan
Marquette University, michael.ryan@marquette.edu

Journal of Physical Chemistry : A, Vol. 124, No. 49 (November 2020): 10225-10238. DOI.

Ion Pairing versus Solvation of Dinitrobenzene Anions in Room-Temperature Ionic Liquids (RTILs): Vibrational Signatures of RTIL–Substrate Interactions

Abderrahman Atifi
Chemistry Department, Marquette University, Milwaukee, Wisconsin
Piotr J. Mak
Chemistry Department, Marquette University, Milwaukee, Wisconsin
Michael D. Ryan
Chemistry Department, Marquette University, Milwaukee, Wisconsin

Abstract

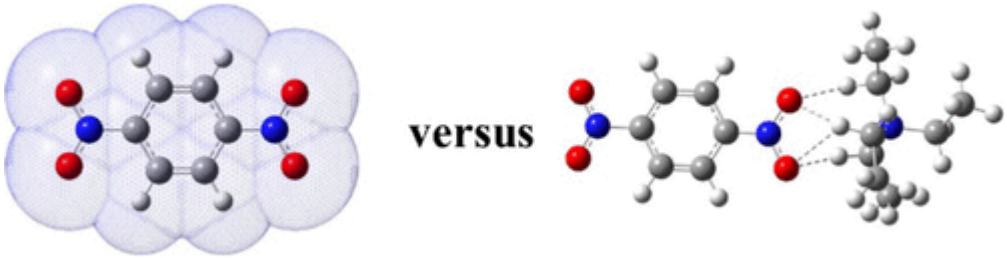

The mechanism of solvation of ions by ionic liquids is more complex than solvation in most molecular solvents as the ionic liquid itself provides the counter ion. Solvation and ion pairing of anionic substrates in room-temperature ionic liquids (RTILs) were investigated using resonance Raman spectroscopy and DFT calculations. The purpose of this study was to differentiate between the formation of discrete cation/anion structures and a double-layer cloud of counter ions without specific atomic interactions between the ionic species. In acetonitrile/RTIL mixtures, the radical anion and dianion of dinitrobenzene (DNB) are stabilized by RTILs through solvation and ion pairing. The formation of the lowest-energy ion pair led to the largest shifts in the Raman band in $DNB^{-\cdot}$, while significantly smaller shifts were predicted for general solvation. The effect of general solvation and ion pair formation was studied using DFT with the implicit solvation model. Identification of the bands most sensitive to tight ion pairing allowed for the interpretation of the observed vibrational changes. The formation of tight ion pairs between the anionic solutes depends on both cation–solute and RTIL cation–anion interactions. Tight ion pairs were observed in RTILs, but general solvation was also important. This work establishes the advantageous use of vibrational spectroscopy to provide detailed structural information not accessible from voltammetry alone.

Introduction

Ionic liquids have been found to have a significant effect on the redox potentials of electroactive substrates,(1) redox mechanisms,(2) electron transfer kinetics,(3) or facilitation of catalysis.(4) The exact nature of the interactions between the ionic liquid and substrates though is less clear. While the obvious explanation is ion pairing, the importance of ion pairing in room-temperature ionic liquids (RTILs) themselves is still not clear,(5) and an understanding of the importance of ion pairing in RTILs is still evolving. The lifetime of the interactions between a specific anion and cation in RTILs is often short so that one should not interpret the ion pairs as discrete neutral species.(6) Other studies such as the measurement of ionicity(7,8) show the presence of neutral pairs and the correlation of the diffusion of ions as indicating the presence of anion/cation pairs. There is evidence though that charge transfer between the cations and anions reduces the charge on the individual ions.(9) Schwenzer et al.(10) have used molecular dynamics and spectroscopic methods to predict ion pair formation in RTIL systems.

In the classical work by Szwarc,(11) two types of ion pairing were defined: contact or loose ion pairs. Contact ion pairs would favor a defined geometric arrangement between the anion and cation as the elimination of solvent between them allows for direct atomic interactions between the anion and cation. For loose ion pairs, the presence of solvent between the ions prevents such direct atomic interactions, and the arrangement of cations around the anions is best described as an ionic cloud around the anion. For this type of ion pair, a continuum model would best describe the interactions. Formation of tight ion pairs would have the greatest effect on the spectroscopic properties of the substrate,(11) especially the vibrational spectra. In molecular solvents, Ahlberg et al.(12) examined the ion pairing between anionic DNB and sodium/potassium ions in DMF using voltammetry. Little ion pairing was observed between the alkali ions and the radical anion, but the dianion was ion-paired with two alkali ions based on the voltammetry. The ion pairing between $DNB^{-\cdot}/DNB^{2-}$ and 1-butyl-3-

methylimidazolium ($BMIm^+$)/1-butyl-2,3-dimethylimidazolium as BF_4^- salts in DMF was studied by Syroeshkin et al.(13) As with alkali ions, there was a weak association with the radical anion and imidazolium, but a much stronger association with the dianion. They calculated that up to four $BMIm^+$ ions were associated with each dianion. Ion pairing of four cations with a dianion is unlikely but probably indicates the formation of RTIL nanodomains. From voltammetric data, one cannot determine if tight or loose ion pairs are formed.

In pure RTILs, the voltammetric behavior may be due to general solvation of the substrate by the RTIL (loose ion pair), or it might be due to the formation of discrete and relatively long-lasting ion pairs (at least long enough to be observed spectroscopically) with a specific geometric structure and atomic interactions (tight ion pair). For example, the voltammetric reduction of 1,4-dinitrobenzene (DNB) occurs in two one-electron steps in aprotic solvents.(14) In room-temperature ionic liquids (RTILs), it was found that the two one-electron waves collapsed into a single two-electron wave.(1)

In mixed molecular solvent/RTIL solutions, the RTIL will be dissociated at low electrolyte concentrations, and the voltammetric behavior will be like other electrolytes. At higher concentrations of RTILs in molecular solutions, aggregations (nanodomains) will form and the electrogenerated anions will partition between the molecular solvent and RTIL phases.(15) For mixed RTIL/molecular solvents, the formation of nanodomains within the solution provides for a local environment where the solute can be solvated as much as it would be solvated within the pure RTIL.(15−19) The effect of mixed molecular solvent/RTIL solutions on the redox potential of the first and second waves was examined by Atifi and Ryan(15) using visible spectroelectrochemistry. Xie et al.(20) also studied 1,4-dinitrobenzene in an RTIL using cyclic voltammetry and infrared spectroscopy.

Recently, Atifi and Ryan(21) used infrared spectroelectrochemistry to study the reduction of tetracyanoquinodimethane (TCNQ) in mixed molecular/RTIL solutions. The voltammetry showed the presence of ion pairing, especially for the dianion. Infrared studies showed no evidence of tight ion pairing with the radical anion. Tight ion pairing with $TCNQ^{2-}$ was observed though for the NTf_2^- RTIL but not for the BF_4^-/PF_6^- salts. The larger and less symmetrical ions such as NTf_2^- are known to form a looser ion pair structure than the symmetrical ions (e.g., BF_4^- and PF_6^-). In the looser structure, it is easier for the substrate anion to displace the RTIL anion. The results of this and related works(15−18,22) visualized the formation of RTIL nanodomains in the solution, and the redox properties were determined by the solvation environment provided by the nanodomain. The voltammetric data alone though do not provide any information on the specific structure of the anionic substrate within the RTIL (tight versus loose ion pairing).

The effect of ion pairing has been studied computationally by Fry et al. in a series of articles. Fry found that the disproportionation between DNB^{2-} and DNB was driven mostly by solvation rather than ion pairing.(23) Ion pairing between the dianion of DNB and substituted imidazolium was examined by Minami and Fry.(24) Fry reviewed his computational studies of electrogenerated ion pair containing tetraalkylammonium ions.(25) Bird et al.(26) examined the effects of ion pairing on the redox potentials of benzophenone and perylene. DFT methods were found to be moderately successful at describing the ion pairing energies. Lewis et al.(27) used vibrational spectroscopy to look for ion pair formation in lithium bistriflimide solutions. We will also use vibrational spectroscopy (resonance Raman) to find such signatures between the RTIL cation and electrogenerated anions to characterize which vibrational changes are due to general solvation and which are due to tight ion pairing.

To probe solvation versus discrete ion pairing interactions, we will begin by predicting the vibrational spectra using DFT calculations. These results will be used to identify signatures of tight ion pair formation and general solvation to analyze the resonance Raman spectra of $DNB^{-\cdot}$/DNB^{2-} and their ion pairs. The resonance Raman spectra of $DNB^{-\cdot}$ and DNB^{2-} in acetonitrile and various mixtures of RTILs will be obtained. The spectra will then be interpreted in light of the DFT calculations. Finally, the literature values for the infrared spectra for $DNB^{-\cdot}$ and

DNB^{2-} in RTILs will be interpreted in light of our DFT calculations.(20) Resonance Raman spectroscopy is ideal for this study because the absorbance bands of the DNB anion and dianion differ enough so that the resonance Raman spectra for the radical anion and dianion can be obtained free of spectral contributions of each other by the judicious choice of the excitation wavelength, even though both ions are present.

Methods Section

Chemicals

High-purity RTILs 1-butyl-3-methylimidazolium hexafluorophosphate ($BMImPF_6$) and 1-butyl-3-methylimidazolium tetrafluoroborate ($BMImBF_4$) were purchased from Merck and TCI and employed without further purification, except as noted in the text. Ethyldimethylpropylammonium bis(trifluoromethylsulfonyl)imide ($AmNTf_2$), tetrabutylammonium perchlorate (TBAP), tetrabutylammonium borohydride ($TBABH_4$, 98%), and anhydrous acetonitrile (99.8%) were purchased from Sigma-Aldrich Chemical Co.

Instrumentation

Cyclic voltammetry was carried out at a platinum electrode (1.6 mm or 10 μ), and a platinum wire was used as an auxiliary electrode. Potentials were measured relative to the $Ag/AgNO_3$ (in CH_3CN) reference electrode. The radical anion of DNB ($DNB^{\cdot-}$) and dianion (DNB^{2-}) were generated by using controlled potential electrolysis. Controlled potential electrolysis was carried out using a homemade small-volume cell. A gold mesh was used as a working electrode, silver wire as a pseudoreference, and platinum wire as an auxiliary electrode. The two compartments were separated by a glass frit. While stirring the solution, electrolysis was carried out by setting the electrode at the potential appropriate to generate $DNB^{\cdot-}$ or DNB^{2-}. The measurements were carried out using a Model 600D Series Electrochemical Analyzer/Workstation (CHI Version 12.06). Resonance Raman (rR) experiments were carried out using excitation lines at 406 and 442 nm for $DNB^{\cdot-}$ and DNB^{2-}, respectively. The 406.7 nm excitation line was provided by a Kr^+ laser (Coherent Innova Sabre Ion Laser), while the 441.6 nm excitation line was obtained from a He-Cd laser (Kimmon Koha Co., Ltd.). The rR spectra of all samples were measured using a Spex 1269 spectrometer equipped with a Spec-10 LN-cooled detector having 2048 pixels (Princeton Instruments, NJ). The laser power was kept at ∼1 mW and the measurements were done using a 180° backscattering geometry using a cylindrical lens to minimize sample heating. The total collection time of each spectrum was 10 min. The slit width was set at 150 μm and the 1200 g/mm grating was used; the linear reciprocal dispersion is 0.655 nm/mm near 400 nm, corresponding to 0.46 cm^{-1}/pixel. The spectra were calibrated with fenchone (Sigma-Aldrich, WI) and processed with Grams/32 AI software (Galactic Industries, Salem, NH).

Procedures

For electrochemical experiments, all solutions were prepared and filled into cells in the glovebox under an argon environment. Tetrabutylammonium perchlorate was used as electrolyte in molecular solvent experiments. For mixtures of molecular/RTIL solvents, a total volume of 0.3–0.5 mL was used for voltammetry. The solutions were prepared using a micropipette. Acetonitrile was used as received. Water was removed from the RTIL by passing N_2 over the solvent, which was heated at 70 to 90 °C. The amount of water in the RTIL was measured by monitoring the stripping peak on a gold electrode due to water. Substantial reduction in the water concentration was obtained as shown by the complete disappearance of the water stripping peak.

Computational Methods

Electronic structure and vibrational spectral calculations were carried out using the m06 functionals and the TZVP basis set, except as noted in the text, using the Gaussian 16 suite of programs.(28) All calculations converged using the tight optimization criteria. Only fundamentals were calculated. Solvation effects were

calculated in Gaussian 16 using the pcm(29) and smd methods.(30,31) In calculating the solvation effect, the structures were first calculated in the gas phase. Then, the structures were reoptimized using the appropriate solvent. NBO analysis was carried out using Gaussian 16. No scaling of the vibrational bands was carried out for these calculations.

Results and Discussion

Cyclic Voltammetry of 1,4-Dinitrobenzene in Acetonitrile/BMImPF$_6$ Mixtures

The cyclic voltammetry of DNB in the presence of BMImPF$_6$ is shown in Figure 1. As was observed previously, the difference between the first redox potential (E°$_1$) and second redox potential (E°$_2$) decreased significantly as the %RTIL increased.(15) From Figure 1, the two waves began to collapse around 15% BMImPF$_6$. The radical anion solutions that were used for resonance Raman spectroscopy were generated coulometrically in acetonitrile where the disproportionation reaction was minimal (about 2% of the radical). When the RTILs were added, disproportionation became more significant. Based on the voltammetric data,(15) about 17% of the radical anion would be lost to disproportionation at 5% RTIL, rising to 50% at 50% RTIL. The visible spectroelectrochemistry of DNB has been previously reported.(15) In acetonitrile, the visible band for DNB$^{\cdot-}$ was observed at 402 nm, which shifted to 448 nm for DNB^{2-}.(15) In BMImPF$_6$, the band for DNB$^{\cdot-}$ shifted slightly to 398 nm, while DNB^{2-} red-shifted to 454 nm. In general, RTILs had a small but measurable effect on the visible spectra of DNB$^{\cdot-}$ and DNB^{2-}.

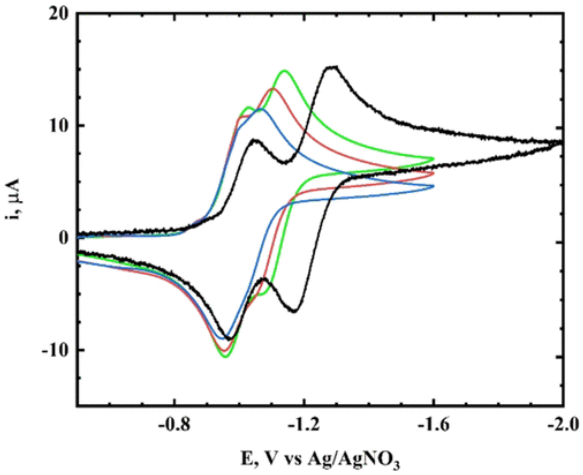

Figure 1. Cyclic voltammetry of 1.0 mM 1,4-DNB in THF and BMImPF$_6$. %BMImPF$_6$: 0%, black; 5%, green; 10%, red; 15%, blue. Scan rate: 100 mV/s. TBAP (0.10 M).

DFT Calculations for DNB

The first step in differentiating tight ion pairing from general solvation by an ionic liquid is to identify spectral signatures of these two types of ionic interactions. Vibrational spectroscopy should be useful in this regard as tight ion pairing would be expected to change the charge distribution in the anionic species, leading to vibrational changes. In addition, tight ion pairing may change the symmetry of the species, leading to some infrared-only active modes becoming both infrared- and Raman-active. To identify these signatures, the DFT spectra of DNB, DNB$^{\cdot-}$, and DNB^{2-} were calculated, taking into account general solvation (using pcm and smd methods) and discrete ion pairing.

Methods such as pcm or smd do not involve specific orientation of the substrate/solvent molecules, as would be seen in a tight ion pair. The general solvation methods would be expected to have less influence on the vibrational spectra as the interactions will be averaged over the entire range of orientations, while the tight ion

pair model could lead to significant changes in the vibrations due to coupling between two or more chemical species. Smaller changes though may occur for symmetrical tight ion pairs. It will be the aim of this work to separate changes due to general solvation from the formation of a tight ion pair structure.

To understand the vibrations of the anions, we need to characterize the neutral species. The DFT calculations and displacement vectors for DNB using the m06 functional/TZVP basis set are shown in Figure 2 and Table 1 for the seven Raman vibrations between 1000 and 1800 cm^{-1} and several important infrared vibrations. Understanding the infrared bands will be important for the analysis of the tight ion pair spectra as the decrease in symmetry of the ion pairs can cause some infrared modes to become Raman-active.

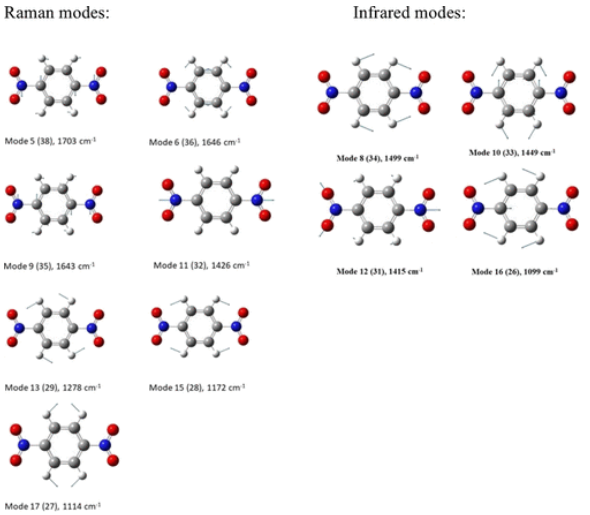

Figure 2. Displacement vectors for DNB using m06/TZVP DFT calculations with mode numbers from Andreev et al.(32) Energies are for the gas-phase species (the mode numbers in parentheses were obtained from the Gaussian results).

Table 1. Experimental and Calculated Values for Raman and Selected Infrared Bands for DNB in Acetonitrile, $BMImBF_4$, and the Gas Phase and Using the pcm Method

mode from Andreev et al.[a]	ν, exp (cm^{-1})[b,c] (symmetry)	$\nu_{neutral}$, DFT, Andreev et al.[a,c]	gas phase, this work[d] (cm^{-1})	acetonitrile (cm^{-1})[d,e]	$BMImBF_4$ (cm^{-1})[d,e]
5 (R)	(b_{3g})	1698	1703	1686 (−17)	1687 (−16)
6 (R)	1590 (a_g)	1681	1646	1645 (−1)	1645 (−1)
8 (IR)	1556 (b_{2u})	1602	1499	1497 (−2)	1497 (−2)
9 (R)	1535 (b_{3g})	1498	1643	1614 (−29)	1618 (−25)
10 (IR)	1378 (b_{2u})	1488	1449	1448 (−1)	1448 (−1)
11 (R)	1358 (a_g)	1471	1426	1425 (−1)	1425 (−1)
12 (IR)	1339 (b_{1u})	1417	1415	1406 (−9)	1407 (−8)
13 (R)	1287 (b_{3g})	1294	1278	1283 (+5)	1272 (−6)
15 (R)	1165 (a_g)	1169	1172	1173 (+1)	1174 (+2)
16 (IR)	1106 (b_{1u})	1119	1099	1099 (0)	1099 (0)
17 (R)	1108 (a_g)	1118	1114	1114 (0)	1115 (+1)

[a]Ref (32); R = Raman band; IR = infrared band.

[b]Experimental values and mode assignments from ref (33).

[c]Scaled by the following equation: ν = 0.8952 ν(6-31G) + 10.2.

[d]Unscaled, m06/TZVP.

[e]Shifts from values in the gas phase in parentheses, m06/TZVP.

The Raman and infrared spectra for DNB have been previously reported by Green and Lauwers.(33) The molecular symmetry of DNB is D_{2h}, which has 42 fundamental modes. Within the spectral region examined in this work (1100–1800 cm^{-1}), there are seven Raman bands (four a_g and three b_{3g}). Four infrared modes (b_{1u} and b_{2u}) in this region will be also examined to compare with literature values of the radical anion and dianion obtained using infrared spectroelectrochemistry because some infrared modes will become Raman-active when the ion pair is formed. Andreev et al.(32) used Hartree–Fock and 6-31G/6-31G** level of computation to predict the vibrations using DFT. Their scaled results are shown in Table 1, along with the correlation between the calculated and experimental bands. While there was general agreement between us and Andreev et al., there were some differences (Table 1), such as the ordering of the energy between the Raman and infrared bands. For consistency with the literature, we will use Andreev et al.'s mode assignments.

The symmetry assignment for each mode studied is also given in Table 1 from Green and Lauwers.(33) In their analysis, the highest-energy experimental band (1590 cm^{-1}) was thought to be a degenerate band; this is unlikely as the vibrational modes are quite different. It is more likely that the weak band calculated to be 1703 cm^{-1} in our work was probably too weak to be experimentally observed. Data for the anion and dianion would be more consistent with this assignment. An examination of the motions showed that modes 5, 9, and 11 had significant movement in the nitro groups, while the motion was primarily in the aromatic ring for modes 6, 13, 15, and 17 (modes 15 and 17 also had small nitro motion). While the energies for the Raman and resonance Raman spectra should be the same, the intensities of the resonance Raman spectra are difficult to calculate. Thus, weak Raman modes should not be automatically excluded as they may become sufficiently enhanced to be seen in the resonance Raman spectra.

The effect of general solvation was calculated using DFT and the pcm (Table 1)/smd (Table S1) methods for acetonitrile and $BMImBF_4$. There was little difference in the predicted Raman bands between the pcm and smd methods. Addition of solvation led to a larger Mulliken negative charge on the oxygen atoms compared to the gas-phase species. The effect of solvation on the Raman spectra was not significant for the totally symmetric modes (a_g) with shifts equal to less than 1 cm^{-1}, while the b_{3g} modes showed larger shifts (5 cm^{-1} or more).

DFT Calculations for $DNB^{-\cdot}$

The results of the DFT calculations for the Raman bands of $DNB^{-\cdot}$ in the gas phase are shown in Table 2. The pcm values for $DNB^{-\cdot}$ in acetonitrile and $BMImBF_4$ are also shown in Table 2 (smd in Table S1). Both small downshifts and upshifts were observed due to solvation. The largest Raman downshift was once again for b_{3g} mode 9, where the gas phase value of 1483 cm^{-1} downshifted to 1444 cm^{-1} for pcm (1453 cm^{-1} for smd). Other than that mode, the shifts for a_g and b_{3g} modes upon solvation were similar and small (±5 cm^{-1}) (Table 2). For the infrared modes, mode 12 was the most affected by solvation, with the gas-phase band downshifting from 1286 cm^{-1} to 1193 cm^{-1} in acetonitrile. While the gas-phase and solution-phase modes are similar, there was significant dampening of the oxygen motion in the solvated species. In other structures to come, we will see the motions of mode 12 to be more variable than other modes. In comparing the pcm values with the smd values, the values were quite similar, except for modes 9 and 13 where significantly larger shifts were predicted for the smd method.

Table 2. Experimental and Calculated Values for Raman and Selected Infrared Bands for $DNB^{-\cdot}$ in Acetonitrile, $BMImBF_4$, and the Gas Phase and Using m06/TZVP and the pcm Method

mode[b]	ν_{anion}, exp[a]	ν_{anion}, DFT, gas phase (cm^{-1})	acetonitrile (cm^{-1})[c]	$BMImBF_4$ (cm^{-1})[c]	$\Delta\nu_{reduction}$[a], DFT (exp) (cm^{-1})
5 (R)	1607	1583	1587 (+4)	1586 (+3)	–99 (–79)[d]
6 (R)	1624	1648	1646 (−2)	1647 (−1)	+1 (+34)
8 (IR)		1472	1476 (+4)	1476 (+4)	

9 (R)	1488	1483	1444 (−38)	1448 (−34)	−170 (−47)
10 (IR)		1383	1377 (+6)	1378 (+5)	−71 (−)
11 (R)	1430	1411	1407 (−4)	1408 (−3)	−18 (+72)
12 (IR)	1210[e]	1286	1193f (−93)	1199 (−87)	−213 (−)
13 (R)	1290	1271	1276 (+5)	1275 (+4)	−7 (+3)
15 (R)	1264	1198	1193f (−5)	1193 (−5)	+20 (+99)
16 (IR)	1056[e]	1143	1092 (−51)	1105 (−38)	−7 (−)
17 (R)		1102	1105 (+3)	1104 (+2)	−9 (−)

[a]Values in acetonitrile; $\Delta\nu_{reduction} = \nu_{DNB^{-\cdot}}$ in acetonitrile – ν_{DNB} in acetonitrile.

[b]R = Raman; IR = infrared.

[c]Shifts from values in the gas phase in parentheses.

[d]Using the calculated DFT value for DNB.

[e]Ref (20), infrared bands.

[f]These bands have coincidentally nearly the same energy but are different modes.

The DFT-predicted changes in each mode upon reduction in acetonitrile are shown in Table 2 and also pictorially in Figure S1. There are three Raman modes that have significant C–NO_2 motion (modes 5, 9, and 11). In acetonitrile, modes 5 and 9 downshifted upon reduction (mode 5: 1686 to 1587 cm^{-1}; mode 9: 1614 to 1444 cm^{-1}) (Tables 1 and 2). The 1425 cm^{-1} band (mode 11), which has considerable C–N motion as well as N–O motion, has a predicted downshift of only 18 cm^{-1} (1425 to 1407 cm^{-1}). The three remaining bands had relatively small predicted shifts with the 1283 cm^{-1} (mode 13) and 1114 cm^{-1} (mode 17) bands downshifting, while the 1173 cm^{-1} band (mode 15) was upshifted (Table 2).

These shifts are consistent with the bonding changes predicted by NBO analysis. In DNB, the N–O bond has roughly a 1.5-bond order, and the C–N bond is a single bond. Upon reduction, a formal π-bond is formed between the C–N atoms and the delocalized π-bonds between N and O disappeared. Because of partial occupancy of the π*-orbital between C and N, the C–N bond is less than a double bond. The consequences of these bonding changes are that reduction weakens the N–O bonds but strengthens the C–N bond, as can be seen by the changes in modes 5, 9, and 11. The strengthening of the C–N bond led to the small downshift of mode 11. These bonding changes are consistent with a quinoidal resonance structure for the radical anion.

The calculated DFT spectra for $DNB^{-\cdot}$ in different environments are plotted in Figure 3A. The gas-phase and pcm solvation spectra gave rise to spectra that are qualitatively similar (the spectra were normalized so that they all appear at roughly the same scale), with generally small upshifts and downshifts due to changes in solvation from acetonitrile and the RTIL (a large shift though was observed for mode 9 between the gas and solvated species). The shifts in the Raman modes for $DNB^{-\cdot}$ as the solvation environment was changed can be seen in Figure 3B.

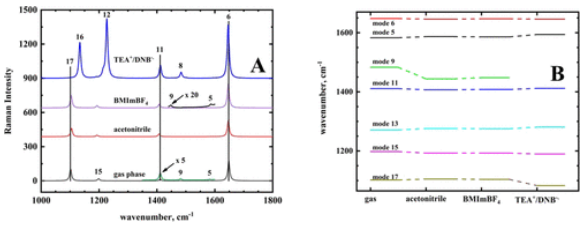

Figure 3. (A) DFT-calculated spectra for $DNB^{-\cdot}$ in the gas phase (gray), acetonitrile (red), $BMImBF_4$ (magenta), and $DNB^{-\cdot}/TEA^+$ ion pair in RTIL (blue). Gas-phase and $BMImBF_4$ spectra expanded by 5× and 20×, respectively, in selected regions. (B) Shifts in the DFT-calculated Raman modes for the gas, solvated, and $TEA^+/DNB^{-\cdot}$ ion pair species in $BMImBF_4$.

The DFT structures for TEA^+ and $BMIm^+$ ion pairs with $DNB^{\cdot-}$ are shown in Figure 4A,B. The structures represent the lowest-energy configurations of the ion pairs. As will be seen later, not all structures converged to a single configuration, which indicated that there was sometimes a shallow energy well, leading the cation to migrate to different positions on the anion. The $DNB^{\cdot-}/TEA^+$ ion pair shows that the hydrogen atoms carrying positive Mulliken charges interacted strongly with the negatively charged oxygens of the nitro group (Figure 4A). The structure of $DNB^{\cdot-}/TEA^+$ is consistent with the work of Fry,(25,34,35) who showed the strong interaction between the positive α-protons and the oxygens of the nitro group. As was observed by Fry, the tetraalkylammonium ion assumed a pseudoplanar conformation when interacting with the anion. The ion pair structure for the $BMIm^+$ ion pair also shows strong charge interactions between the positive atoms of the cation and the negative atoms of anion radical (Figure 4B). The structure shows that hydrogen bonding and π–π interactions between the imidazolium ring and the π-system of the nitro groups are not as important. As with TEA^+, it is primarily charge interactions in the $BMIm^+$ ion pair that dominate the ion pair formation.

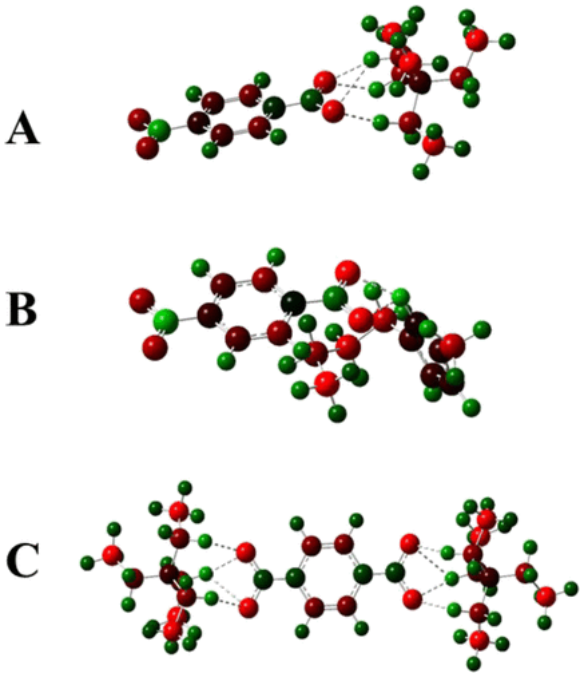

Figure 4. (A) DFT structure of $DNB^{\cdot-}/TEA^+$. (B) DFT structure of $DNB^{\cdot-}/BMIm^+$. (C) DFT structure of $DNB^{2-}/2\ TEA^+$. Mulliken charges: positive, green; negative, red.

The structures in Figure 4 should not be interpreted as crystal structures. There are other local minima that can exist between the DNB anion and cation. Repeating the calculations for Figure 4A where we move the initial structure significantly from the calculated minimum, the structure tends to iterate to Figure 4A (e.g., by increasing the anion/cation distance, moving the cation above/below the anion plane). It is possible to iterate to other structures if the cation is moved directly above the C–N bond (Figure S2A). In the gas phase, this structure is 24 kJ higher in energy than the structure in Figure 4A, but the energy difference becomes negligible using acetonitrile/pcm calculation. In the RTIL, the energetics of this structure is probably unfavorable as such an ion pair would push the RTIL anion close to the negatively charged oxygens of the nitro groups. This structure (Figure S2) though did not converge when solvation is used, with the cation moving around above the nitro group. It is the aim of this work to differentiate between tight and loose ion pairs, rather than determining the exact ion pair structure. Figure S2 shows that other configurations are possible, but the vibrational shifts on their formation are similar.

Spectral analysis of the ion pairs is more complex than the free ion due to changes in symmetry when the ion pair is formed. With the formation of an ion pair with the radical anion, the D_{2h} symmetry is lost, and the comparison of the modes is approximate. In many cases, the direction of the atomic motion for the modes is the same, but the size of the displacements can change. The Raman mode displacements are shown in Figure S3 ($BMIm^+$ ion pair) and Figure S4 (TEA^+ ion pair). For example, the size of the displacements of mode 5 in Figure 2 is different from mode 5 in Figure S3, but the direction of the displacements is similar. In some cases, the changes are large enough to change the Raman activity of the mode. Modes that were omitted in Tables S2–S4 have generally changed so much that they are no longer Raman-active.

The DFT-calculated vibrational bands for TEA^+ and $BMIm^+$ ion pairs with $DNB^{\cdot-}$ in an RTIL are given in Table 3 (DFT values in the gas phase and acetonitrile phase are given in Table S2). The shifts in the Raman modes upon formation of an ion pair are shown in Figure 3B (mode 9 displacements were not observed for the ion pair). Only small differences were observed in the calculated band for the ion pairs between the acetonitrile and RTIL solvents (Table S2), though larger shifts were observed in going from the gas phase to the solvated phase. The magnitude of the shifts due to ion pairing was sensitive to the distance between the anion and cation, as measured by the nitro-oxygen to the nearest cation proton distance. In the gas phase, the average distance between the nitro-oxygen and nearest cation proton of TEA^+ was 2.169 Å. In acetonitrile, the distance increased to 2.350 Å and tightened somewhat in the RTIL solvent (2.329 Å). This was reflected in the vibrational spectra as the largest shifts from the free ion were for the gas-phase species, and the smallest shifts were for the acetonitrile-solvated species, with the RTIL-solvated ion pair in between but closer to the acetonitrile species. In interpreting the experimental spectra, we should keep this uncertainty (ion pair distance) in mind. The smd method leads to similar shifts for the $TEA^+/DNB^{\cdot-}$ ion pair as the pcm method.

Table 3. DFT and Experimental Modes for the Ion Pair of $DNB^{\cdot-}$ Using m06/TZVP in $BMImBF_4$ (pcm Method)

mode [a]	$Am^+/DNB^{\cdot-}$ ion pair[b], ν_{exp} (cm^{-1})	$TEA^+/DNB^{\cdot-}$ ion pair[b,c], ν_{DFT} (cm^{-1})	$BMIm^+/DNB^{\cdot-}$ ion pair[b], ν_{exp} (cm^{-1})	$BMIm^+/DNB^{\cdot-}$ ion pair[b,c], ν_{DFT} (cm^{-1})
5 (R)	1636	1594 (+8)	1638	1594 (+8)/1592
6 (R)	1624	1646 (−1)	1623	1644 (−3)
8 (IR)	1488	1483 (+7)	1490	1484 (+8)
9 (R)				
10 (IR)	1365	1369 (−9)	1370	1363 (−15)
11 (R)	1400	1412 (+4)/1411	1400	1411 (+3)/1417
12 (IR)	1230	1227 (+28)		1238 (+39)
13 (R)	1300	1281 (+6)	1300	1281(+6)
15 (R)	1269	1190 (−3)	1270	1189 (−4)
16 (IR)		1134 (+29)		1141 (+36)
17 (R)		1083 (−21)		1080 (−24)

[a]R = Raman; IR = infrared.

[b]All modes in the column are Raman-active.

[c]Shifts from $DNB^{\cdot-}$ in $BMImBF_4$ in parentheses.

The spectra of the TEA^+ and $BMIm^+$ ion pairs in RTILs are similar, with slightly larger shift for the $BMIm^+$ ion pairs in most cases (Table 3). The vibrational modes should split due to the decreased symmetry of the ion pair, as compared to the free anion. In particular, the two Raman ν_{NO2} modes (modes 5 and 11) should split in the ion pair. This can be seen for the $BMIm^+$ ion pair with mode 5 bands at 1592 and 1594 cm^{-1} and mode 11 at 1411 and 1417 cm^{-1}. Smaller splittings were seen for the TEA^+ ion pair, with mode 5 splitting being too small to be seen. These results show though that the ion pair interaction is relatively weak, and we have focused on the modes most similar to the free ion or new modes that yield stronger Raman bands. The Raman spectrum for the

$TEA^+/DNB^{\cdot-}$ ion pair (RTIL solvation) is shown in Figure 3A. Our discussion will focus on the TEA^+ ion pair while making note of the $BMIm^+$ ion pair when there are differences or when their modes are relevant to the discussion. The effect of other ion pair structures on the Raman spectrum is shown in Figure S2B. The shifts from the free ion upon the formation of the ion pair are all in the same direction as observed for the structure in Figure 4A, with most of the shifts being smaller than Figure 4A but several were larger. In addition, it is likely that the shifts in the solution phase will be smaller than in the gas phase (as was observed for the structure in Figure 4A). In all, there are probably other local minima, but these structures should only affect the size of the shift, but not the direction.

There are significant changes in the Raman spectrum of the ion pair from the solvated free anion. The first striking feature of the ion pair Raman spectrum is the strong intensities of formerly infrared-only modes (8, 12, and 16). In the free ion, the vibrations were either Raman- or infrared-active, making the analysis straightforward. With the decrease in symmetry, most modes were both Raman- and infrared-active, meaning that modes that were not seen in the free ion could be observed in the ion pair (Table 3). In fact, modes 8, 12, and 16 are some of the strongest bands in the calculated spectrum (Figure 3A) (this may not be true for the resonance Raman spectrum). The displacements for mode 9 in the free anion were not observed in the ion pair. In the solvated ion pair, coupling between the anion and cation was strong for mode 9, and the most similar mode was mostly infrared-active. Overall, large shifts were predicted for modes 5 and 9 (gas phase), but only small shifts were predicted for modes 6, 11, and 17. The upshift in mode 5 is probably the best signature of the formation of the ion pair of the radical anion $DNB^{\cdot-}$. Similar results were obtained for the $TEA^+/DNB^{\cdot-}$ ion pair using the smd method.

DFT Calculations for DNB^{2-}

DFT calculations for DNB^{2-} in the gas phase were carried out, and the seven Raman modes between 1050 and 1700 cm^{-1} are summarized in Table 4, along with some infrared modes. Calculations for solvation effects on the dianion were carried out using the smd (Table S1) and pcm (Table 4) methods. For acetonitrile, the predicted shifts using pcm and smd were quite similar; the smd method predicted, in most cases, larger shifts than the pcm method in $BMImBF_4$. The displacements in mode 9 of the dianion were more like $DNB^{\cdot-}$ than DNB. The largest downshifts were observed for mode 5 (−97 cm^{-1}) and mode 9 (−144 cm^{-1}). These modes have significant N–O motion, and the N–O bond lengths increased from 1.208 to 1.247 Å, a weakening of the N–O bond. Smaller downshifts upon reduction were seen for modes 13, 15, and 17 (Figure S1). Two bands though were upshifted (mode 6: +13 cm^{-1}; mode 11: +79 cm^{-1}). Mode 11 has significant C–N motion, and this bond became stronger upon reduction (1.405 Å to 1.357 Å). The solvent environment had little effect on the Raman bands as the solvent was changed from acetonitrile to $BMImBF_4$ (Table 4). Except for mode 9, the shifts upon solvation were similar for a_g and b_{3g} modes.

Table 4. Experimental and Calculated Values for Raman and Selected Infrared Bands for DNB^{2-} in Acetonitrile, $BMImBF_4$, and the Gas Phase and Using the pcm Method

mode[b]	$\nu_{dianion}$, exp	$\nu_{dianion}$, DFT, gas phase	$\nu_{dianion}$, DFT, acetonitrile (cm^{-1})[c]	$BMImBF_4$ (cm^{-1})[c]	$\Delta\nu_{reduction}$[a], DFT (exp) (cm^{-1})
5 (R)	1469	1479	1490 (+11)	1489 (+10)	–97 (−138)
6 (R)	1572	1652	1659 (+7)	1659 (+7)	+13 (−52)
8 (IR)	1464[d]	1471	1468 (−3)	1468 (−3)	
9 (R)		1318	1300 (−18)	1302 (−16)	–144 (–)
10 (IR)		1395	1389 (−6)	1389 (−6)	
11 (R)	1423	1476	1486 (+10)	1486 (+10)	+79 (−7)
12 (IR)	1356[d]	1369	1333 (−36)	1337 (−32)	
13 (R)	1247	1256	1250 (−6)	1250 (−6)	–26 (−43)

15 (R)	1147	1179	1170 (−9)	1172 (−7)	−23 (−117)
16 (IR)	1056[d]	1108	1072 (−36)	1078 (−30)	
17 (R)	1110	1082	1083 (+1)	1083 (+1)	−22 (−)

[a]$\Delta\nu_{reduction}$ = ν_{DNB2-} in acetonitrile – $\nu_{DNB-\cdot}$ in acetonitrile.

[b]R = Raman; IR = infrared.

[c]Shifts from values in the gas phase are shown in parentheses.

[d]Ref (20).

The DFT calculations for an ion pair with DNB^{2-} and two TEA^+ ions were also carried out. The structure is shown in Figure 4C and the displacement vectors are shown in Figure S5. With the second ion, the structure of the dianion was more symmetrical, and the ion pair returned to pseudo-D_{2h} symmetry (some differences in the cation structure would prevent strict D_{2h} symmetry). These differences in cation structure should have little effect on the anionic vibrations. The mode symmetries from Table 1 should apply for the dication ion pair. The DFT calculations were carried out in the gas phase and in the solution phase (acetonitrile and RTIL). The results are shown in Table 5 (for acetonitrile) and Table S2.

Table 5. DFT and Experimental Modes for the Ion Pair of DNB^{2-} Using m06/TZVP in Acetonitrile (pcm Method)

mode[a]	DNB^{2-} ion pair bands in RTILs[b], ν_{exp} (cm^{-1})	TEA^+/DNB^{2-} ion pair[c,d], ν_{DFT} (cm^{-1})	2 TEA^+/DNB^{2-} ion pair[d], ν_{DFT} (cm^{-1})
5 (R)	1471 (+3)	1497 (+7)	1500 (+11)
6 (R)	1589 (+17)	1661 (+2)	1661 (+2)
8 (IR)	1469 (+1)	1464 (−4)	1478 (+10)[d]
9 (R)		1307 (+7)	1294 (−6)
10 (IR)		1390 (+1)	1389 (0)[d]
11 (R)		1509 (+23)/1498	1489 (+3)
12 (IR)	1357 (+1)	1338 (+5)	1346 (+13)
13 (R)	1282 (+35)	1268 (+18)	1249 (−1)
15 (R)	1165 (+18)	1171 (+1)	1172 (+2)
16 (IR)			1071 (−1)
17 (R)	1110 (0)	1098 (+7)	1083 (0)

[a]R = Raman; IR = infrared.

[b]Values in parentheses are the shifts from DNB^{2-}.

[c]All modes in the column are Raman-active.

[d]Shift from DNB^{2-} in acetonitrile in parentheses.

The largest shifts from the free anion were observed for the gas phase, and the shifts decreased significantly as the ion pair was solvated. These changes were consistent with the structural changes. In the gas phase, the average distance between the nitro-oxygens and the nearest hydrogens of the cation increased from 2.053 Å to 2.253 Å in acetonitrile. In the gas phase, as was observed for the radical anion, formation of the neutral ion pair of the dianion led to an upshift in the Raman bands from the free dianion, except for mode 9 (Table S2). DFT calculations of the tight ion pair of DNB^{2-} with two $BMIm^+$ ions in the gas or solution phase did not converge. This was probably also due to the shallow energy well for the tight ion pair as the $BMIm^+$ cations tended to migrate around the nitro group.

The shifts for the Raman modes from the DFT-calculated spectra for the TEA^+ ion-paired species are shown in Table 5 and visualized in Figure S6. For the neutral dication ion pair, the calculated shifts between the solvated and ion-paired species are generally relatively small (mode 6: +2 cm^{-1}; mode 9: −6 cm^{-1}; mode 11: +3

cm^{-1}; mode 13: −1 cm^{-1}; mode 15: +2 cm^{-1}; mode 17: 0 cm^{-1}). A significant shift was only seen for mode 5 (+11 cm^{-1}). This is due to the symmetrical nature of the dication complex where the ionic forces tended to cancel themselves. For diagnostic purposes, one should look for shifts in modes 5 and 6 for evidence of the dication ion pair formation.

Analysis of the DNB^{2-} ion pairs is more complex than the radical anion because the monocation ion pair is also possible. The bands for the monocation of DNB^{2-} are summarized in Table 5 for acetonitrile solvation. As with the radical anion ion pair, the monocation ion pair with DNB^{2-} loses its D_{2h} symmetry, and the issue of mode identification is the same as with the $DNB^{-\cdot}$ ion pair. Values for the gas-phase and RTIL solvation are given in Table S2. Most of the vibrational shifts are small except for modes 5, 9, 11, and 13. The solvated species (acetonitrile and RTIL) gave very similar spectra but were much less shifted than the gas-phase species. As with the radical anion ion pair, the splitting of mode 5 was too small to be observed, while two bands could be observed for mode 11. As with the other ion pairs, significant loosening of the ion pair occurred upon solvation with the nitro-oxygen to cation hydrogen distance increasing from 1.956 Å to 2.230 Å in acetonitrile (2.199 Å in RTIL). As with the radical anion ion pair, the loss of symmetry led to infrared bands becoming Raman-active and vice versa. These new bands may make the monocation more visible in the Raman spectra because of the lack of interference from the free dianion and dication ion pair where the infrared bands are not Raman-active.

Resonance Raman Spectra of Dinitrobenzene Anion and Dianion

The resonance Raman spectrum of $DNB^{-\cdot}$ in acetonitrile is shown in Figure 5 (black trace). Six major bands were observed at 1264, 1290, 1430, 1488, 1607, and 1624 cm^{-1} (band at 1558 cm^{-1} was present in all spectra and was not a fundamental band of $DNB^{-\cdot}$). The seventh band (mode 17) was outside the observed spectral region. The appearance of six resonance Raman bands indicated that there was significant enhancement of both the a_g and b_{3g} modes. Significant enhancement for the b_{3g} modes can occur if there was efficient coupling of nearby electronic states with the b_{3g} modes.(36) The assignments for most of the modes are straightforward and are given in Table 2 and Figure 5. The assignments of the highest-energy bands at 1607 and 1624 cm^{-1} are less clear. Both bands have a strong intensity in the resonance Raman spectra, while only one a_g mode occurs in that region; the b_{3g} mode though is close in energy. The behavior of these bands in the presence of the RTILs will help us identity to them. From the DFT calculations, mode 6 is insensitive to ion pair formation, with the DFT calculations predicting minimal shifts (Table 3). On the other hand, mode 5 is predicted to upshift by 8 cm^{-1} upon formation of the ion pair. As will be discussed below, these behaviors are the most consistent with mode 5 being the 1607 cm^{-1} band and mode 6 occurring at 1624 cm^{-1}.

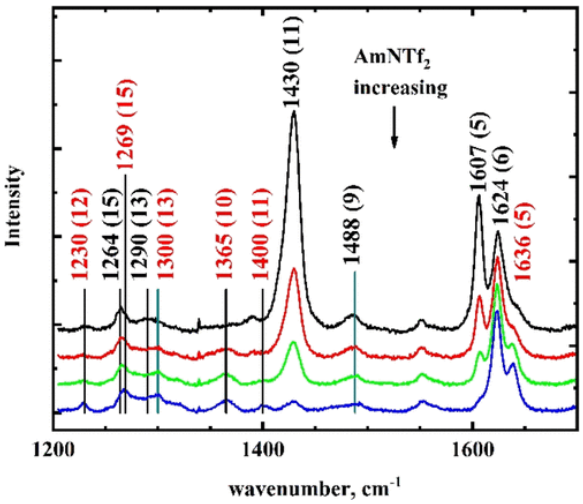

Figure 5. Resonance Raman spectra of $DNB^{-\cdot}$ in acetonitrile and mixed acetonitrile/$AmNTf_2$ solutions. %$AmNTf_2$ in acetonitrile: 0% $AmNTf_2$, black; 5% $AmNTf_2$, red; 20% $AmNTf_2$, green; 50% $AmNTf_2$, blue. Black

labels: $DNB^{-\cdot}$; red labels: ion pair bands. The intensities of the spectra were normalized versus the 1624 cm^{-1} band. The numbers in parentheses are mode numbers. The spectra were measured using the 406.7 nm excitation line.

For ease of comparison, the Raman bands in Tables 1, 2, and 4 are summarized in Table 6 for the three oxidation states of DNB. As predicted, we see that modes 5 and 9 showed the largest downshifts upon reduction (mode 5 downshifted by 79 cm^{-1} using the DFT-calculated value of 1686 cm^{-1} for DNB; mode 9 downshifted by 47 cm^{-1}). These downshifts are less than the values predicted by DFT (mode 5: 99 cm^{-1}; mode 9: 170 cm^{-1}). The remaining band with significant nitro motion is mode 11, where only an 18 cm^{-1} downshift is predicted, while the observed value was a 72 cm^{-1} upshift. These results (and the other that follows) indicate that DFT calculations predict too much weakening of the N–O bands and strengthening of the C–N bond upon reduction.

Table 6. Shifts in the Resonance Raman Bands of DNB Species in Acetonitrile upon Reduction

mode	band	DNB exp (DFT) (cm^{-1})	$DNB^{-\cdot}$ exp (DFT) (cm^{-1})	DNB^{2-} exp (DFT) (cm^{-1})
5	b_{3g}	(1686)	1607 (1587)	1469 (1490)
6	a_g	1590 (1645)	1624 (1646)	1572 (1659)
9	b_{3g}	1535 (1614)	1488 (1444)	(1300)
11	a_g	1358 (1425)	1430 (1407)	1423 (1486)
13	b_{3g}	1287 (1283)	1290 (1276)	1247 (1250)
15	a_g	1165 (1173)	1264 (1193)	1147 (1170)
17	a_g	1108 (1114)	(1105)	1110 (1083)

As $AmNTf_2$ was added to the solution (Figure 5), shifts were observed in the position and intensity of the bands. To assess the spectral changes clearly, all spectra were normalized versus the 1624 cm^{-1} band. DFT calculations showed that this band was the least affected by solvation and ion pairing. The most notable qualitative feature of Figure 5 as $AmNTf_2$ was added was the decrease in intensity of the spectra relative to the 1624 cm^{-1} band. The 1430 cm^{-1} band nearly disappeared as compared to the 1624 cm^{-1} band, as did several other bands.

The loss in intensity of the spectra is consistent with the formation of a tight ion pair, which is less symmetrical than the free anion. Assignment of the ion pair bands is given in Table 3. From Figure 5 (ion pair bands have red labels), we can see that the mode 5 band (1607 cm^{-1}) upshifted to 1636 cm^{-1} (Table 3), eventually replacing the 1607 cm^{-1} band. The shift was somewhat larger than the DFT-predicted value of 8 cm^{-1} but was in the same direction. In addition, there was a significant weakening of the intensity of the band. DFT calculations have shown that an upshift in mode 5 (1607 cm^{-1} in acetonitrile) was indicative of the formation of a tight ion pair. Mode 6 (1624 cm^{-1}) was not shifted by the formation of the ion pair as predicted. New bands were observed at 1230 and 1365 cm^{-1}, which were assigned to modes 12 and 10, respectively, which were infrared modes, which became Raman-active in the ion pair. Mode 11 dropped considerably in intensity relative to the 1624 cm^{-1} band and downshifted to 1400 cm^{-1} (DFT: 1412 cm^{-1}). There was still some residual acetonitrile-solvated radical anion left as can be seen by the weak band remaining at 1430 cm^{-1}. Modes 13 and 15 had small upshifts. DFT predicted a small upshift for mode 13 but a small downshift for mode 15. Overall, the analysis does show that the observed bands correspond well with the DFT-calculated values (Table 3), and the changes in the intensity of the bands and the size and direction of the observed shifts support the formation of a tight ion pair over solvation in $AmNTf_2$.

The experiment was repeated using $BMImBF_4$ as the RTIL (Figure 6). In comparing Figure 5 ($AmNTf_2$) with Figure 6 ($BMImBF_4$), there were qualitative similarities. In both cases, the 1607 cm^{-1} band (mode 5) decreased relative to the 1624 cm^{-1} band (mode 6), and a new mode 5 band at 1636 cm^{-1} appeared. The 1430 cm^{-1} band (mode 11) decreased in intensity relative to the 1624 cm^{-1} band. Mode 15 (1264 cm^{-1}) and mode 13

(1290 cm^{-1}) shifted in a manner similar to Figure 5. But, at 50% $BMImBF_4$, both bands due to mode 5 could still be observed, and the 1430 cm^{-1} band still had considerable intensity. Clearly, in $BMImBF_4$, a considerable fraction of the radical anion did not form a tight ion pair.

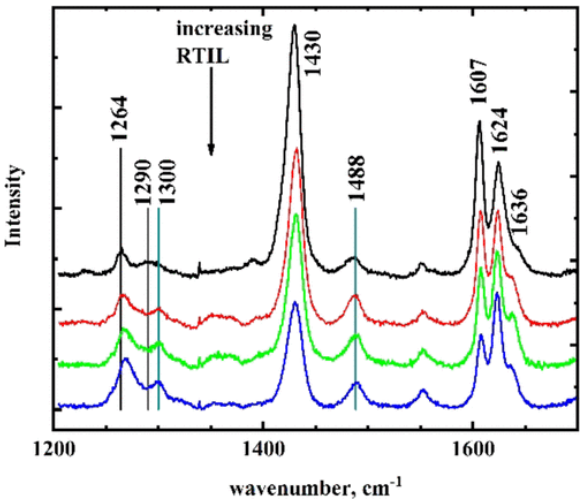

Figure 6. Resonance Raman spectra of $DNB^{\cdot-}$ in acetonitrile and mixed acetonitrile/$BMImBF_4$ solutions. %$BMImBF_4$ in acetonitrile: 0% $BMImBF_4$, black; 5% $BMImBF_4$, red; 20% $BMImBF_4$, green; 50% $BMImBF_4$, blue. All spectral intensities normalized to the 1624 cm^{-1} band. The spectra were displaced downward for better viewing. The spectra were measured using the 406.7 nm excitation line.

To see the radical anion ion pairing in the RTIL more clearly, the acetonitrile species was subtracted from the 50% $BMImBF_4$ spectrum. The result is shown in Figure 7 (red trace, assuming that $DNB^{\cdot-}$ in acetonitrile was 38% of the original concentration). The spectrum of the remaining species can now be seen more clearly, with bands occurring at 1270, 1300, 1370, 1400, 1436, 1490, 1611, 1623, and 1638 cm^{-1}. In the same figure, the spectrum for the radical anion in 50% $AmNTf_2$ is also shown. The bands due to the tight ion pair of $DNB^{\cdot-}$ with the $BMIm^+$ cation can be observed in the subtracted spectrum of $BMImBF_4$ (1270, 1300, 1370, 1400, 1490, and 1638 cm^{-1}). The 1400 and 1638 cm^{-1} bands have been assigned as the ion pair bands for modes 11 and 5, respectively.

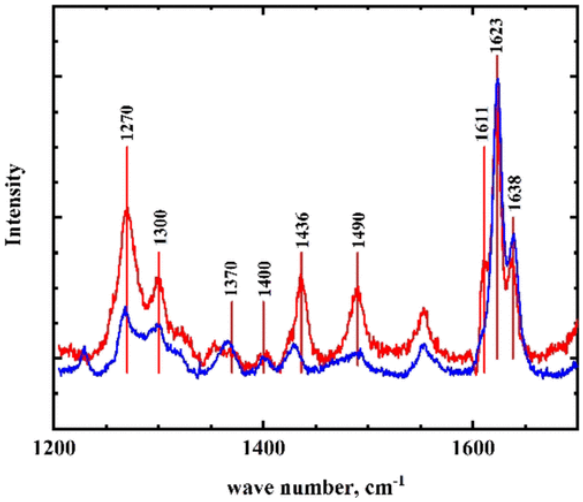

Figure 7. (A) Deconvoluted $DNB^{\cdot-}/BMImBF_4$ spectrum assuming the 38% $DNB^{\cdot-}$ presence for 50% $BMImBF_4$ (red). (B) Spectrum of $DNB^{\cdot-}$ in 50% $AmNTf_2$ (blue). Both spectra taken in acetonitrile.

The 1400 cm^{-1} band is probably broadened due to the two overlapping bands for mode 11, which are due to the decreased symmetry of the ion pair as compared to the free ion. In addition, there is a band at 1436 cm^{-1}, which is due to the RTIL-solvated mode 11 band. Thus, two bands due to the solvated species (1430 and 1436 cm^{-1}) are present at 50% $BMImBF_4$ along with the ion pair band at 1400 cm^{-1}. Similarly, for mode 5, the acetonitrile-solvated species (1607 cm^{-1}) and RTIL-solvated species (1611 cm^{-1}) were observed along with the ion pair band at 1638 cm^{-1}. The fact that the 1436 cm^{-1} band was not observed in the $AmNTf_2$ spectra, and the much less intense residual acetonitrile band at 1430 cm^{-1} showed that, in $AmNTf_2$, the $DNB^{\cdot-}$ species was either ion-paired (1400 cm^{-1}) or acetonitrile-solvated (1430 cm^{-1}).

Tian and Jin(37) observed infrared bands for $DNB^{\cdot-}$ in acetonitrile at 1210 and 1056 cm^{-1}. Later work by Xie et al.(20) showed bands for $DNB^{\cdot-}$ in $BMImBF_4$ at 1218 and 1056 cm^{-1}. Gas-phase DFT calculations for $DNB^{\cdot-}$ predicted strong infrared bands at 1383 cm^{-1} (mode 10), 1286 cm^{-1} (mode 12), 1143 cm^{-1} (mode 16), and 995 cm^{-1} (mode 21). Using the pcm solvation model in acetonitrile ($BMImBF_4$), these bands dropped in energy to 1377 (1378), 1193 (1199), 1092 (1105), and 991 (991) cm^{-1} (Figure S7). The two strongest infrared bands and DFT-calculated bands for $DNB^{\cdot-}$ are 1193 cm^{-1} (mode 12) and 1092 cm^{-1} (mode 16), which can be correlated to the experimental 1210 and 1056 cm^{-1} bands, respectively. Mode 12, according to Andreev et al.'s assignment, gave a band for DNB at 1339 cm^{-1} (predicted, 1406 cm^{-1}), which dropped to 1210 cm^{-1} upon reduction (predicted, 1193 cm^{-1}). This constituted a downshift of 129 cm^{-1} upon reduction, which is consistent with reduction on the nitro group. The band at 1106 cm^{-1} (mode 16) in DNB downshifted to 1056 cm^{-1} upon reduction compared to a 7 cm^{-1} downshift predicted in the DFT calculations.

The DFT-calculated infrared spectrum for $DNB^{\cdot-}$ with the $BMIm^+$ ion pair spectra is shown in Table 3 and Figure S7 (blue trace). In the ion pair spectrum, the strongest bands in the infrared between 900 and 1300 cm^{-1} are at 956, 1080, 1141, 1189, and 1238 cm^{-1}. The 956 cm^{-1} band is a cation mode with no anion motion. The 1080 cm^{-1} band contains both anion and cation motions, with the anion mode being most similar to mode 17, a Raman band in the free anion. The band at 1189 cm^{-1} has motion similar to mode 15. This band is strongly infrared- and Raman-active. Mode 16, which can be observed in the infrared spectra of the free radical anion, was calculated to occur at 1141 cm^{-1} but was strongly Raman-active in the ion pair with weak infrared activity. Therefore, the infrared band observed at 1056 cm^{-1} (mode 16) for $DNB^{\cdot-}$ was predicted to shift to 1133 cm^{-1} in the ion pair. Mode 12, which was predicted to be 1193 cm^{-1} (infrared) in the free anion, was calculated to be 1227 cm^{-1} in the ion pair (Raman/infrared, upshift of 28 cm^{-1} from the solvated radical anion). This band was observed at 1230 cm^{-1} in the resonance Raman spectra (Figure 5), indicating the presence of the ion pair species. The infrared changes are consistent with an RTIL-solvated radical anion spectrum (transfer from acetonitrile to RTIL: exp, 8 cm^{-1}; DFT, 6 cm^{-1}). No upshift was observed for the 1056 cm^{-1} band going from acetonitrile to $BMImBF_4$, while a 13 cm^{-1} upshift was predicted.

Based on the resonance Raman and infrared spectra, mixtures of $BMImBF_4$ and acetonitrile are consistent with a mixture of acetonitrile/RTIL-solvated and ion-paired species. The small observed upshift in the infrared spectra was consistent with RTIL-solvated $DNB^{\cdot-}$. The ion-paired $DNB^{\cdot-}$ was probably not visible in the infrared spectra due to the overlap of those bands with the solvent but was seen in the Raman spectra (1230 cm^{-1}). Because of the transparency of the solvent in resonance Raman spectroscopy, both acetonitrile- and RTIL-solvated bands (e.g., 1607/1611 cm^{-1}) and ion pair band (1636 cm^{-1}) were observed. The ion pairs were probably present in the RTIL nanodomain. As the RTIL is added to acetonitrile, previous work has shown that the aggregations grew rapidly, while the concentration of the cation in the molecular phase reached a saturation value.(38) These results are consistent with the ion pair species being in the RTIL nanodomain. The infrared spectroelectrochemistry of DNB was probably limited by solvent absorption, though this issue was not addressed by the authors. Because of the solvent, it was difficult to observe the same mode for both the

oxidized and reduced species, as well as the solvated and ion pair species. The small shifts due to solvation were more consistent with the pcm method than the smd method, which predicted some large shifts (Table S1).

The resonance Raman spectrum for DNB^{2-} in acetonitrile is shown in Figure 8 (black trace). The assignments of the resonance Raman bands of DNB^{2-} are given in Tables 4 and 6, along with the experimental and predicted shifts upon reduction of the radical anion. The resonance Raman bands for DNB^{2-} along with the modes are given in black in Figure 8. The first point of note is that the choice of excitation energy allowed the observation of DNB^{2-} with no interference of the $DNB^{\cdot-}$ species. In particular, the strongest bands of $DNB^{\cdot-}$ (1430, 1607, and 1624 cm^{-1}) were not observed in the DNB^{2-} spectra (Figure 8). Similarly, the strongest DNB^{2-} bands (1423 and 1572 cm^{-1}) were not seen in the $DNB^{\cdot-}$ spectra (Figure 5). Unlike the radical anion spectrum, the a_g modes dominated the resonance Raman spectra of the dianion (modes 6, 11, 15, and 17). The b_{3g} modes were weak (modes 5 and 13) or not observed (mode 9). While one might be tempted to assign the weak band at 1665 cm^{-1} to mode 6 (as predicted by DFT), this would be inconsistent with it being a strong a_g mode. This band is probably a combination or overtone band.

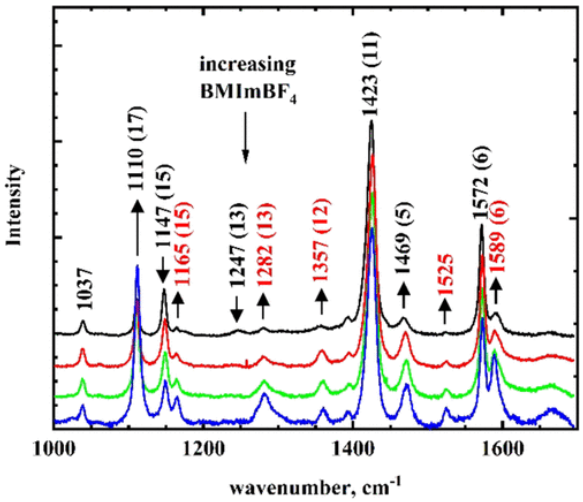

Figure 8. Resonance Raman spectra of DNB^{2-} in acetonitrile and mixed acetonitrile/$BMImBF_4$ solutions. %$BMImBF_4$ in acetonitrile: 0% $BMImBF_4$, black; 5% $BMImBF_4$, red; 20% $BMImBF_4$, green; 50% $BMImBF_4$, blue. Spectral intensities are normalized to the 1572 cm^{-1} band. Values in parentheses are the vibrational modes. Labels in black are dianion bands; labels in red are ion pair bands. The spectra were measured using the 441.6 nm excitation line.

As with the radical anion, changes were observed with the addition of $BMImBF_4$ (Figure 8). Ion pair bands are shown in red. Several minor bands in the acetonitrile spectrum due to electrolyte ion pairing increased significantly when $BMImBF_4$ was added. In particular, the 1525, 1357, 1282, and 1165 cm^{-1} bands, which were barely visible in acetonitrile, became prominent bands with the RTIL present. Unlike the radical anion, the spectra of all three RTILs are quite similar (Figure S8, $BMImPF_6$; Figure S9, $AmNTf_2$). A comparison of the three RTILs at their highest concentrations is shown in Figure S10.

In comparing the calculated and observed bands from the DNB spectra as the molecule is reduced, we can see some deviations from the expected results. Notably, for mode 11, the trend (DFT in parentheses) was 1358 cm^{-1} (1425 cm^{-1}) for the neutral ion, 1430 cm^{-1} (1407 cm^{-1}) for $DNB^{\cdot-}$, and 1423 cm^{-1} (1486 cm^{-1}). The shifts between the neutral ion and dianion between the experimental values (65 cm^{-1}) and DFT values (61 cm^{-1}) were consistent, though the actual experimental values were higher than the DFT-calculated values. On the other hand, the difference between the DFT-calculated values and experimental values was the smallest for $DNB^{\cdot-}$ (DFT: 1407 cm^{-1}; experimental: 1430 cm^{-1}). Mode 11 involves C–N and N–O stretching and these results would

indicate that the DFT calculations predicted these bonds to be stronger than was experimentally observed for DNB and DNB^{2-}. Similarly, the trend for mode 6 does not follow the values predicted by the DFT calculations. The DFT calculations predicted a gradual increase in the energy of the modes upon reduction (neutral ion: 1645 cm^{-1}; radical anion: 1646 cm^{-1}; dianion: 1659 cm^{-1}). The observed values were 1590 cm^{-1} (neutral ion), 1624 cm^{-1} (radical anion), and 1572 cm^{-1}. As with mode 11, the smallest difference between the DFT and observed values was for $DNB^{\cdot-}$ (1624 cm^{-1} versus 1646 cm^{-1}). Larger deviations were seen for DNB and DNB^{2-}, with the DFT values being higher in energy than the observed values. Mode 6 has significant C–C and C–N stretching motion. The C–N stretching motion is in common between these two modes, indicating that the C–N bond is weaker than predicted by DFT. Using resonance theory, this would indicate that the DFT calculation overestimates the quinoidal contribution to the overall structure in DNB and DNB^{2-}.

The agreement between theory and experiment was the best for Mode 5. DFT calculations predicted 1587 cm^{-1} for $DNB^{\cdot-}$ and 1490 cm^{-1} for DNB^{2-} versus experimental values of 1607 and 1469 cm^{-1}, respectively (the experimental value for DNB is not known). Mode 9 was weak and not observed in the $DNB^{\cdot-}$ and DNB^{2-} spectra. Modes 13 and 15 downshifted as predicted by DFT (DFT: −26 and −23 cm^{-1}), but the experimental shifts were larger (−43 and −117 cm^{-1}). While some deviations were observed between the experimental and DFT-calculated spectra of the free ion, formation of ion pairs shifts the bands in a predictable manner. The size of the shift will depend on the distance between the anion and cation, but the direction of the shifts can generally be predicted by DFT calculations, even when there are larger deviations for the free ion.

With the addition of RTILs, three possible species can be formed: solvated DNB^{2-}, monocation, and dication ion pair. An examination of Table 4 predicted only small changes as the solvation changes from acetonitrile to the RTIL, except for the infrared modes 12 and 16 (+4 and +6 cm^{-1}, respectively). The remaining bands shifted by 2 cm^{-1}, at most. For the dication ion pair, significant shifts were calculated in the Raman spectra for modes 5 and 9 and in the infrared region for modes 8 and 12 (Table 5). The remaining bands are close to the acetonitrile values. For the monocation, significant shifts were calculated for modes 5, 8, 9, 11–13, and 17 (Table 5). In addition, several infrared bands become Raman-active due to the symmetry of the monocation ion pair.

The assignment of the new experimental bands in the RTILs is given in Table 5. Because of the failure of the dication pair to converge in $BMImBF_4$, the DFT values in Table 5 use the acetonitrile values. The monocation ion pairs of $DNB^{\cdot-}$ and DNB^{2-} did converge in the RTIL, and the results differed very little from acetonitrile. Therefore, the use of acetonitrile values should not significantly affect our conclusions. The new bands (shown in red in Figure 8) in the presence of the RTIL could represent the dication, monocation ion pair, or solvated DNB^{2-}.

Modes 6 and 15 showed the largest shifts upon the addition of the RTILs. For mode 6, DFT calculations showed a small upshift upon forming the ion pair as compared to the free ion. The predicted shifts though were quite dependent on the tightness of the ion pair, and the larger observed upshift may be due to a tighter ion pair. In the gas phase, the distance between the ions was the shortest and the upshift was the largest (8 cm^{-1}). The shift in mode 6 was consistent with a tighter ion pair in the RTIL than predicted. Mode 5 shift upshifted by about 3 cm^{-1}, a little smaller than 7–11 predicted by DFT calculations. Bands at 1165 and 1282 cm^{-1} were assigned to modes 15 and 13 of the monocation ion pair (only small upshifts were predicted for the dication ion pair), which would be an upshift of 18 and 35 cm^{-1}. The DFT-predicted upshifts were 1 and 18 cm^{-1}. Additional new bands were observed at 1165, 1282, 1357, and 1525 cm^{-1}. A band at 1357 cm^{-1} was assigned to mode 12. This band is infrared-active in the free ion but Raman-active for the monocation ion pair. In the free dianion, mode 12 was previously observed at 1356 cm^{-1} in the infrared.(37) More discussion of these modes will be delayed until the discussion of the literature infrared values. The identity of the 1525 cm^{-1} band is unclear; from DFT calculations, the most likely bands would be the strong infrared and Raman bands at 1502 and 1514 cm^{-1} in the monocation

DNB^{2-} ion pair. This band contained both anion and cation motions, and the mode is unique to the monocation ion pair.

From this assignment, ion pair bands were also observed in the acetonitrile spectrum. This is consistent with formation of ion pairs with the electrolyte cation (TBA^+). The asymmetrical shape of the Raman band at 1589 cm^{-1} in acetonitrile indicates the presence of more than one species. As the RTIL is added to the solution, the band became more symmetrical. The difference spectrum between acetonitrile and 5% $BMImBF_4$ is shown in Figure 9A. Several of the resonance Raman bands increased in intensity in the presence of the RTIL. Also notable in the difference spectrum were the small upshifts at 1147 cm^{-1} (mode 15), 1423 cm^{-1} (mole 11), and 1572 cm^{-1} (mode 5). These shifts are consistent with small shifts in the modes due to the change in solvation from acetonitrile to $BMImBF_4$, which was predicted by the pcm method. Figure 9B shows that a new band at 1596 cm^{-1} was observed when the 1589 cm^{-1} band was removed. DFT calculations (Table 5) predicted similar upshifts for both the dication and monocation ion pair. This shoulder at 1596 cm^{-1} disappeared at high concentrations of the RTIL, which would be consistent with the 1589 cm^{-1} band due to the dication ion pair. These results are consistent with the infrared spectroelectrochemistry of $TCNQ^{2-}$ in acetonitrile/RTIL, where general solvation and tight ion pairs were observed depending on the RTIL.(21) Unfortunately, one cannot calculate quantitatively the concentration ratios of general solvation to ion pairs based on intensity ratios because the Raman enhancements for each species may be different.

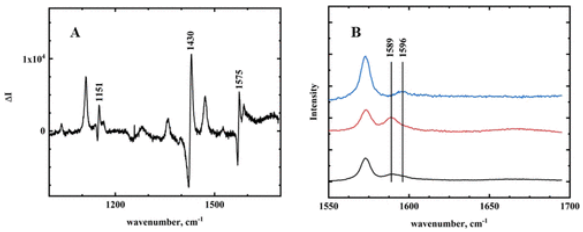

Figure 9. (A) Difference in the resonance Raman spectra between 5% $BMImBF_4$ in acetonitrile and acetonitrile alone from Figure 8. (B) Black trace: resonance Raman spectrum of DNB^{2-} in 5% $BMImBF_4$ in acetonitrile. Red trace: resonance Raman spectrum of DNB^{2-} in 50% $BMImBF_4$ in acetonitrile. Blue trace: subtraction of 1589 cm^{-1} band in black trace (5%) from red trace (50%).

Tian and Jin(37) also examined the second reduction of DNB in acetonitrile using infrared spectroelectrochemistry. Infrared bands were observed at 1464, 1356, and 1056 cm^{-1}. DFT calculations showed three strong infrared bands at 1468 cm^{-1} (mode 8), 1333 cm^{-1} (mode 12), and 1072 cm^{-1} (mode 16) (DFT values were calculated using the pcm method for acetonitrile, Table 4). Xie et al.(20) found that the 1464 and 1356 cm^{-1} infrared bands (modes 8 and 12, respectively) shifted to 1472 and 1364 cm^{-1} in $BMImBF_4$ (8 cm^{-1} upshift for both bands). Mode 12 was also observed in the resonance Raman spectra at 1357 cm^{-1}, which can only be due to the monocation ion pair due to symmetry reasons. DFT calculations (Table 5) predicted an upshift of 5 cm^{-1} for the monocation from acetonitrile-solvated DNB^{2-} for modes 12 (1 cm^{-1} observed). An upshift of 13 cm^{-1} was predicted in going from the acetonitrile- to RTIL-solvated dication DNB^{2-} ion pair. For solvation changes alone, a shift of +4 cm^{-1} (mode 12) was predicted. While the infrared spectra showed only a single absorbance for modes 8 and 12, the low spectral resolution of the data (16 cm^{-1}) makes it impossible to determine from the infrared data whether the RTIL-solvated and monocation ion pairs are present in the solution. Mode 16 at 1072 cm^{-1} is unchanged in the infrared spectra in changing the solvent from acetonitrile to the RTIL. DFT calculations predict an upshift of 1 cm^{-1} with the formation of the dication ion pair and an upshift of 6 cm^{-1} with general solvation changes. Mode 16 was not found in the monocation ion pair.

Modes 12 and 16 were also observed in the infrared radical anion spectrum, while mode 8 was not observed. Upon reduction, mode 12 was observed to upshift from 1210 cm^{-1} in the radical anion to 1356 cm^{-1} (DNB^{2-}) in

the infrared (DFT: $\Delta\nu$ = +140 cm^{-1}). Mode 8 was not observed in the radical anion spectrum but was predicted to occur at 1476 cm^{-1} in acetonitrile. This would correspond to a downshift of 12 cm^{-1} (DFT: 8 cm^{-1}). Mode 16 was unchanged upon the reduction of $DNB^{\cdot-}$ to DNB^{2-} in acetonitrile versus a predicted downshift of 20 cm^{-1}.

From the vibrational spectra, we can summarize the equilibria involving the RTIL and the anions of DNB. For $AmNTf_2$, which has an asymmetrical anion, $DNB^{\cdot-}$ is tightly ion-paired in the RTIL nanodomain as $DNB^{\cdot-}$ was able to displace the NTf_2^- anion. At 50% RTIL, there is some residual $DNB^{\cdot-}$ remaining in acetonitrile but no observable free $DNB^{\cdot-}$ in the RTIL nanodomain (1430 cm^{-1} reflected acetonitrile nanodomain; 1436 cm^{-1} indicated the RTIL nanodomain). For $BMImBF_4$/$BMImPF_6$, which contained symmetrical anions, which ion-pair strongly with $BMIm^+$, $DNB^{\cdot-}$ formed ion pairs with the $BMIm^+$ cation, but also, there was some free $DNB^{\cdot-}$ in the RTIL nanodomain. In addition, there was a significant amount of $DNB^{\cdot-}$ in the acetonitrile nanodomain, as indicated by modes 5 and 11.

For DNB^{2-}, the difference spectrum in Figure 9 showed small but significant upshifts in modes 15, 11, and 6, indicating transfer of DNB^{2-} from acetonitrile to the RTIL nanodomain even at low concentrations of the RTIL. Unlike $DNB^{\cdot-}$, the spectra for DNB^{2-} were nearly the same for all the RTILs studied, both with symmetrical and asymmetrical anions. The unsymmetrical nature of the monocation ion pair made identification of this species easier in the Raman spectra as some infrared modes for DNB^{2-} became Raman-active. The correspondence between the literature infrared bands and new resonance Raman bands helped identify these modes. Mode 6 showed that solvent-solvated, monocation, and dication ion pairs were present in the RTIL. The other Raman modes were insensitive to the difference between solvent-solvated and ion pair species. The infrared mode 12, when combined with the resonance Raman spectra, showed that the mono- and dication ion pairs were formed in the RTIL.

The result of this work provides insight into the formation of ion pairs due to the reduction of electroactive substrates in solution. The work of Xie et al.(20) and others showed that the shift in the second wave of DNB was consistent with the formation of an ion pair with two $BMIm^+$ species. While some tight ion pairing was observed in Figure 8, a significant amount of the dianion was not in a tight ion pair (mode 6 showed a strong band for the solvent-solvated species). Ion pairing of the dianion was consistent with loose ion pairs where there was an ionic cloud around the anion, with some tight ion pairing. Without spectroscopic signatures, it is not possible to determine the type of ion pair structure from voltammetric data alone. For catalysis, one would expect tight ion pairs to stabilize high-energy intermediates (e.g., $CO_2^{\cdot-}$) better than general solvation. This work and our previous work(21) show that RTILs with larger, asymmetric anions (e.g., NTf_2^-) are better able to form tight ion pairs with anionic substrates than smaller symmetrical anions (e.g., BF_4^- or PF_6^-).

Conclusions

The results of this work allowed us to interpret the vibrational spectral features of the anion and dianion in the RTIL/acetonitrile mixtures in terms of general solvation and discrete ion pair formation. Because the resonance Raman spectra are not affected by solvent absorption, more bands were able to be observed than were seen by infrared spectroelectrochemistry. In combination with DFT calculations, it was possible to determine which shifts are due to general solvation and which are due to the formation of ion pair structures. This was especially important for the $BMImBF_4$ RTIL where both generally solvated anionic species and ion pairs were present.

The resonance Raman results show that the radical anion and dianion of DNB form ion pairs with RTILs that contain Am^+ and $BMIm^+$ cations in mixed molecular solvent/RTIL solutions. While tetraalkylammonium cations formed a stronger ion pair with $DNB^{\cdot-}$ than $BMIm^+$, this was probably related to competition between $DNB^{\cdot-}$ and the RTIL anion. The voltammetric data confirmed that the formation of ion pairs between $DNB^{\cdot-}$ and Am^+ or $BMIm^+$ is small, but at high concentrations of the RTIL, essentially all the radical anion species were ion-paired

with $AmNTf_2$. At 50% $BMImBF_4$, significant amounts of ion pairing were observed, but there were also indications of the RTIL-solvated anion.

This work shows the importance of DFT calculations to identify signatures of ion pair formation. Especially for the symmetrical ion pairs, few of the bands were sensitive to ion pairing. By identifying the ion pair-sensitive bands, researchers can focus on those modes that are most indicative of structure. In addition, it is important to use solvation with DFT calculations of ion pairs as measurable shifts were observed from the gas-phase calculations, even for ion pairs.

Supporting Information

The Supporting Information is available free of charge at https://pubs.acs.org/doi/10.1021/acs.jpca.0c06267.

- Tables for solvent corrections of vibrational bands, resonance Raman spectra of DNB^{2-}, displacement vectors for ion pairs, and calculated infrared $DNB^{-\cdot}$ spectra https://epublications.marquette.edu/chem_data/4/ (PDF)

Terms & Conditions

Notes

The authors declare no competing financial interest.

Acknowledgments

The authors would like to thank James R. Kincaid for the use of his Raman instruments for this work and for consultations with him during the revision.

References

1 Fry, A. J. Strong ion-pairing effects in a room temperature ionic liquid. *J. Electroanal. Chem.* **2003**, *546*, 35– 39, DOI: 10.1016/S0022-0728(03)00143-8

2 Sun, L.; Ramesha, G. K.; Kamat, P. V.; Brennecke, J. F. Switching the reaction course of electrochemical CO_2 reduction with ionic liquids. *Langmuir* **2014**, *30*, 6302– 6308, DOI: 10.1021/la5009076

3 Tanner, E. E. L.; Foong, K. Y.; Hossain, M. M.; Batchelor-McAuley, C.; Aldous, L.; Compton, R. G. The Corannulene Reduction Mechanism in Ionic Liquids is Controlled by Ion Pairing. *J. Phys. Chem. C* **2016**, *120*, 8405– 8410, DOI: 10.1021/acs.jpcc.6b02551

4 Rosen, B. A.; Salehi-Khojin, A.; Thorson, M. R.; Zhu, W.; Whipple, D. T.; Kenis, P. J. A.; Masel, R. I. Ionic Liquid-Mediated Selective Conversion of CO_2 to CO at Low Overpotentials. *Science* **2011**, *334*, 643– 644, DOI: 10.1126/science.1209786

5 Kirchner, B.; Malberg, F.; Firaha, D. S.; Hollóczki, O. Ion pairing in ionic liquids. *J. Phys.: Condens. Matter* **2015**, *27*, 463002, DOI: 10.1088/0953-8984/27/46/463002

6 Zhang, Y.; Maginn, E. J. Direct Correlation between Ionic Liquid Transport Properties and Ion Pair Lifetimes: A Molecular Dynamics Study. *J. Phys. Chem. Lett.* **2015**, *6*, 700– 705, DOI: 10.1021/acs.jpclett.5b00003

7 Tokuda, H.; Hayamizu, K.; Ishii, K.; Susan, M. A. B. H.; Watanabe, M. Physicochemical Properties and Structures of Room Temperature Ionic Liquids. 2. Variation of Alkyl Chain Length in Imidazolium Cation. *J. Phys. Chem. B* **2005**, *109*, 6103– 6110, DOI: 10.1021/jp044626d

8 Ueno, K.; Tokuda, H.; Watanabe, M. Ionicity in ionic liquids: correlation with ionic structure and physicochemical properties. *Phys. Chem. Chem. Phys.* **2010**, *12*, 1649– 1658, DOI: 10.1039/b921462n

9 Hollóczki, O.; Malberg, F.; Welton, T.; Kirchner, B. On the origin of ionicity in ionic liquids. Ion pairing versus charge transfer. *Phys. Chem. Chem. Phys.* **2014**, *16*, 16880– 16890, DOI: 10.1039/C4CP01177E

10 Schwenzer, B.; Kerisit, S. N.; Vijayakumar, M. Anion pairs in room temperature ionic liquids predicted by molecular dynamics simulation, verified by spectroscopic characterization. *RSC Adv.* **2014**, *4*, 5457– 5464, DOI: 10.1039/c3ra46069j

11 Szwarc, M. Ions and ion pairs. *Acc. Chem. Res.* **1969**, *2*, 87– 96, DOI: 10.1021/ar50015a004

12 Ahlberg, E.; Drews, B.; Jensen, B. S. The effect of alkali metal cations on the cathodic reduction of *p*-dinitrobenzene in DMF. The formation of insoluble triple ions of the dianion with Na^+ and K^+ ions. *J. Electroanal. Chem.* **1978**, *87*, 141– 148, DOI: 10.1016/S0022-0728(78)80389-1

13 Syroeshkin, M. A.; Mendkovich, A. S.; Mikhal'chenko, L. V.; Gul'tyai, V. P. The nature of associates of 1,4-dinitrobenzene dianion with 1-butyl-3-methylimidazolium and 1-butyl-2,3-dimethylimidazolium cations. *Russ. Chem. Bull.* **2009**, *58*, 1688– 1693, DOI: 10.1007/s11172-009-0233-x

14 Maki, A. H.; Geske, D. H. Electron spin resonance (EPR) and polarographic investigation of substituted nitrobenzene negative ions. *J. Am. Chem. Soc.* **1961**, *83*, 1852– 1860, DOI: 10.1021/ja01469a019

15 Atifi, A.; Ryan, M. D. Electrochemistry and Spectroelectrochemistry of 1,4-Dinitrobenzene in Acetonitrile and Room Temperature Ionic Liquids: Ion Pairing Effects in Mixed Solvents. *Anal. Chem.* **2014**, *86*, 6617– 6625, DOI: 10.1021/ac5012987

16 Atifi, A.; Ryan, M. D. Spectroscopic Evidence of Nanodomains in THF/RTIL Mixtures: Spectroelectrochemical and Voltammetric Study of Nickel Porphyrins. *Anal. Chem.* **2015**, *87*, 12245– 12253, DOI: 10.1021/acs.analchem.5b03411

17 Atifi, A.; Ryan, M. D. Influence of RTIL Nanodomains on the Voltammetry and Spectroelectrochemistry Of Fullerene C_{60} in Benzonitrile/Room Temperature Ionic Liquids Mixtures. *Electrochim. Acta* **2016**, *191*, 567– 576, DOI: 10.1016/j.electacta.2016.01.104

18 Atifi, A.; Ryan, M. D. Altering the Coordination of Iron Porphyrins by Ionic Liquid Nanodomains in Mixed Solvent Systems. *Chem. – Eur. J.* **2017**, *23*, 13076– 13086, DOI: 10.1002/chem.201701540

19 Atifi, A.; Keane, T. P.; DiMeglio, J. L.; Pupillo, R. C.; Mullins, D. R.; Lutterman, D. A.; Rosenthal, J. Insights into the Composition and Function of a Bismuth-Based Catalyst for Reduction of CO_2 to CO. *J. Phys. Chem. C* **2019**, *123*, 9087– 9095, DOI: 10.1021/acs.jpcc.9b00504

20 Xie, Y.; Li, D.; Jin, B. In situ FT-IR spectroelectrochemical study of the reduction of 1,4-dinitrobenzene in room-temperature ionic liquids. *J. Electroanal. Chem.* **2016**, *774*, 1– 6, DOI: 10.1016/j.jelechem.2016.04.049

21 Atifi, A.; Ryan, M. D. Voltammetry and Spectroelectrochemistry of TCNQ in Acetonitrile/RTIL Mixtures. *Molecules* **2020**, *25*, 303, DOI: 10.3390/molecules25020303

22 Atifi, A.; Mak, P. J.; Ryan, M. D. Proton-coupled reduction of an iron nitrosyl porphyrin in the protic ionic liquid nanodomain. *Electrochim. Acta* **2019**, *295*, 735– 741, DOI: 10.1016/j.electacta.2018.10.179

23 Fry, A. J. Disproportionation of arene radical anions is driven overwhelmingly by solvation, not ion pairing. *Electrochem. Commun.* **2005**, *7*, 602– 606, DOI: 10.1016/j.elecom.2005.04.007

24 Minami, Y.; Fry, A. J. Computational study of the interactions between electrochemically-generated 1,4-dinitrobenzene dianion and substituted imidazolium ions. *AIP Conf. Proc.* **2007**, *963*, 481– 484, DOI: 10.1063/1.2836117

25 Fry, A. J. When Ions Meet: Computational Studies on the Structure of Electrogenerated Ion Pairs. *Electrochem. Soc. Interface* **2016**, *25*, 37– 40, DOI: 10.1149/2.F04162if

26 Bird, M. J.; Iyoda, T.; Bonura, N.; Bakalis, J.; Ledbetter, A. J.; Miller, J. R. Effects of electrolytes on redox potentials through ion pairing. *J. Electroanal. Chem.* **2017**, *804*, 107– 115, DOI: 10.1016/j.jelechem.2017.09.030

27 Lewis, N. H. C.; Zhang, Y.; Dereka, B.; Carino, E. V.; Maginn, E. J.; Tokmakoff, A. Signatures of Ion Pairing and Aggregation in the Vibrational Spectroscopy of Super-Concentrated Aqueous Lithium Bistriflimide Solutions. *J. Phys. Chem. C* **2020**, *124*, 3470– 3481, DOI: 10.1021/acs.jpcc.9b10477

28 Frisch, M. J.; Trucks, G. W.; Schlegel, H. B.; Scuseria, G. E.; Robb, M. A.; Cheeseman, J. R.; Scalmani, G.; Barone, V.; Petersson, G. A.; Nakatsuji, H.; *Gaussian 16. Rev. B.01*, Wallingford, CT, 2016.

29 Tomasi, J.; Persico, M. Molecular Interactions in Solution: An Overview of Methods Based on Continuous Distributions of the Solvent. *Chem. Rev.* **1994**, *94*, 2027– 2094, DOI: 10.1021/cr00031a013

30 Bernales, V. S.; Marenich, A. V.; Contreras, R.; Cramer, C. J.; Truhlar, D. G. Quantum Mechanical Continuum Solvation Models for Ionic Liquids. *J. Phys. Chem. B* **2012**, *116*, 9122– 9129, DOI: 10.1021/jp304365v

31 Marenich, A. V.; Cramer, C. J.; Truhlar, D. G. Universal Solvation Model Based on Solute Electron Density and on a Continuum Model of the Solvent Defined by the Bulk Dielectric Constant and Atomic Surface Tensions. *J. Phys. Chem. B* **2009**, *113*, 6378– 6396, DOI: 10.1021/jp810292n

32 Andreev, G. N.; Stamboliyska, B. A.; Penchev, P. N. Vibrational spectra and structure of 1,4-dinitrobenzene and its ^{15}N labeled derivatives: an ab initio and experimental study. *Spectrochim. Acta* **1997**, *53*, 811– 818, DOI: 10.1016/S1386-1425(96)01876-8

33 Green, J. H. S.; Lauwers, H. A. Vibrational spectra of benzene derivatives. XIII. Dinitrobenzenes. *Spectrochim. Acta* **1971**, *A27*, 817– 824, DOI: 10.1016/0584-8539(71)80160-5

34 Fry, A. J. Computational Studies of Ion Pairing. 8. Ion Pairing of Tetraalkylammonium Ions to Nitrosobenzene and Benzaldehyde Redox Species. A General Binding Motif for the Interaction of Tetraalkylammonium Ions with Benzenoid Species. *J. Org. Chem.* **2013**, *78*, 5476– 5481, DOI: 10.1021/jo4005958

35 Fry, A. J. Computational Studies of Ion Pairing. 7. Ion-Pairing and Association Effects between Tetraalkylammonium Ions and Nitrobenzene Redox Species. Ion Pairing to Neutral Substances. *J. Org. Chem.* **2013**, *78*, 2111– 2117, DOI: 10.1021/jo302385r

36 Strommen, D. P.; Nakamoto, K. Resonance Raman spectroscopy. *J. Chem. Educ.* **1977**, *54*, 474– 478, DOI: 10.1021/ed054p474

37 Tian, D.; Jin, B. FT-IR spectroelectrochemical study of the reduction of 1,4-dinitrobenzene on Au electrode: Hydrogen bonding and protonation in proton donor mixed media. *Electrochim. Acta* **2011**, *56*, 9144– 9151, DOI: 10.1016/j.electacta.2011.07.088

38 Pádua, A. A. H.; Costa Gomes, M. F.; Canongia Lopes, J. N. A. Molecular Solutes in Ionic Liquids: A Structural Perspective. *Acc. Chem. Res.* **2007**, *40*, 1087– 1096, DOI: 10.1021/ar700050q